Crucial Involvement of the CCR2/CCL2 Interactions in Azoxymethane/Dextran Sodium Sulfate-induced Colon Carcinogenesis in Mice

doi: 10.1007/BF03354226

Crucial involvement of the CCR2/CCL2 interactions in azoxymethane/dextran sodium sulfate-induced colon carcinogenesis in mice

Boryana K. Popivanova, Feodora I. Kostadinova, and Naofumi Mukaida
Division of Molecular Bioregulation, Cancer Research Institute, Kanazawa University, 13-1 Takara-machi, Kanazawa 920-0934, Japan

Abstract

Azoxymethane (AOM) administration followed by repetitive dextran sulfate sodium (DSS) ingestion causes chronic colonic inflammation with macrophage infiltration and enhanced expression of a macrophage-tropic chemokine, CCL2, in wild-type (WT) mice. These mice eventually develop multiple colon tumors. In contrast, mice deficient in CCR2, a specific receptor for CCL2, exhibited less macrophage infiltration and attenuated tumor formation. WT mice transplanted with CCR2-deficient bone marrow developed fewer tumors after AOM and DSS treatment than either WT or CCR2-deficient mice transplanted with WT bone marrow. Furthermore, when injected to WT mice with multiple colon tumors, a CCL2 antagonist expression vector attenuated macrophage and granulocyte infiltration, and eventually reduced the numbers and sizes of tumors. These results implied the crucial involvement of the CCL2-CCR2 interactions in the development and progression of colon carcinoma associated with chronic inflammation.

Introduction

Ulcerative colitis (UC) is an inflammatory bowel disease, characterized by repetitive relapses and remissions, which can cause epithelial dysplasia and can progress to invasive cancer. Thus, long-standing UC is a predisposing factor for colon cancer development. The combined administration of a carcinogen, azoxymethane (AOM) and dextran sulfate sodium (DSS) to rodents is widely employed in order to recapitulate colon cancer associated with chronic inflammation such as UC. DSS causes extensive mucosal inflammatory reaction in the colon, and a prior AOM administration accelerates development of colon carcinomas. In this AOM/DSS-induced colon carcinogenesis, massive intracolonic infiltration of macrophages is consistently observed and is presumed to have a crucial role.

Monocyte chemoattractant protein-1 (MCP-1)/CCL2 is a chemokine which regulates the migration and activation of monocytes/macrophages. It exerts its effects through binding to its specific receptor, CCR2. Accumulating evidence indicates the role of the CCL2/CCR2 axis in various chronic inflammatory diseases, and in cancer pathobiology.

To explore the role of CCL2/CCR2 axis in AOM/DSS-induced colon carcinogenesis, we used CCR2-deficient mice and the gene delivery of an N-terminal deletion mutant of human CCL2 (7ND), which effectively inhibits CCL2 *in vivo* (1). Our experiments revealed that the CCL2/CCR2 interactions induced the recruitment of cyclooxygenase (COX)-2-expressing inflammatory cells, leading to colon cancer development.

Methods

Animal experiments

Pathogen-free 8- to 12-week old female wild-type BALB/c mice (WT) and CCR2$^{-/-}$ mice were injected intraperitoneally with 12 mg/kg body weight of AOM (Sigma-Aldrich, Inc., St. Louis, MO) dissolved in physiological saline. Five days later, 2 % DSS ((MW 36,000-50,000; MP Biochemicals Inc., Aurora, OH) was given in the drinking water over five days, followed by 16 days of regular water. This cycle was repeated a total of 3 times (Fig. 1A). In another series of experiments, human 7ND-expressing- or pcDNA3 vector were injected into the femoral muscle of WT mice at day 56, followed by electroporation with an electrical pulse generator (ECM830; BTX, San Diego, CA) (Fig. 4A). All animal experiments were performed in compliance with the Guideline for the Care and Use of Laboratory Animals of Kanazawa University.

Bone marrow chimeric mice generation

Cell suspensions from male WT or CCR2$^{-/-}$ bone marrow were prepared from femurs and tibias. Female WT or CCR2$^{-/-}$ mice received a single intravenous injection of 1 x 10^7 bone marrow cells, after being irradiated with 4.25 Gy X-rays followed by 4.25 Gy X-rays (MPR-1520R; Hitachi) 4 hours later. The following groups of chimeric mice were generated; WT to WT, WT to CCR2$^{-/-}$, CCR2$^{-/-}$ to WT, and CCR2$^{-/-}$ to CCR2$^{-/-}$ mice.

Histopathological and immunohistochemical analyses of mouse colon tissues

Paraffin-embedded or frozen sections of mouse colon were used for immunohistochemical dectetion of β-catenin-, CCR2-, MCP-1/CCL2-, F4/80-, Ly-6G-, COX-2-, cytokeratin 20-, and CD31-positive cells. Positive cells were enumerated on 5 randomly chosen visual fields at x 400 magnification. The pixel numbers of CD31-positive areas were measured on 5 randomly chosen visual fields at x 200 magnification with the aid of Adobe Photoshop software.

Quantitative RT-PCR analysis

Real-Time PCR was performed on Applied Biosystems StepOne™ Real-Time PCR System using the comparative C_T quantitaion method. TaqMan® Gene Expression Assays (Applied Biosystems, Foster City, CA), containing specific primers (accession numbers: MCP-1/CCL2 – Mm00441242_m1, KC/CXCL1 – Mm00433859_m1, COX-2 –

Mm00478374_m1, GAPDH – Mm99999915_g1) and TaqMan® MGB probe (FAM ™ dye-labeled), TaqMan® Fast Universal PCR Master Mix were used with 10 ng of cDNA to detect and quantify the expression levels of MCP-1/CCL2, KC/CXCL1, and COX-2 in mouse colon tissues.

Statistical analysis

The mean ± S.D. were calculated for all parameters determined. Statistical significance was evaluated using one-way analysis of variance (ANOVA), and *p* values lower than 0.05 were considered statistically significant.

Results

Enhanced CCL2 expression in the colon during the course of colon carcinogenesis

A single intraperitoneal injection of the carcinogen AOM, followed by 3 rounds of 2% DSS intake, induced the development of multiple tumors in the middle to distal colon of WT mice (Fig. 1B, C). Because we previously observed a massive infiltration of macrophages during the course of this colon carcinogenesis process (2), we investigated the expression of the macrophage-tropic chemokine MCP-1/CCL2 and its specific receptor, CCR2. CCL2 mRNA expression level was negligible in untreated WT mice, but DSS intake augmented it (Fig. 1D). CCL2 protein was detected in mononuclear cells infiltrating into lamina propria and submucosal regions, endothelial cells at the earlier phase and colon carcinoma cells at the later phase (data no shown). CCR2 was expressed by mononuclear cells infiltrating the lamina propria and submucosa, and in some colon carcinoma cells during the course of this colon carcinogenesis (data not shown).

Reduction in AOM/DSS-induced inflammatory reaction and subsequent tumor formation in the absence of CCR2

Consistently, microscopical analysis demonstrated that WT mice developed severe inflammation in the middle to distal colon at day 7. At day 14, inflammatory cell infiltration persisted, accompanied with dysplastic glands (data not shown). Moreover, immunohistochemical analysis demonstrated that inflammatory cells consisted of F4/80-positive macrophages and Ly6G-positive granulocytes (Fig.1E, F). At days 28 to 35, adenocarcinomatous lesions with nuclear β-catenin accumulation appeared in the presence of macrophage and granulocyte infiltration, and their sizes and numbers increased progressively, thereafter (Fig.1B, C). On the contrary, $CCR2^{-/-}$ mice displayed mild inflammatory changes in the colon during the course of DSS intake as evidenced by attenuated infiltration of macrophages and granulocytes (Fig.1E, F) and eventually developed few adenocarcinomatous lesions with less nuclear β-catenin accumulation (Fig. 1B, C). These observations implied the CCL2/CCR2 interactions as crucial for the development of chronic inflammation-associated colon carcinoma development.

Contribution of CCR2-expressing bone marrow-derived cells to colon carcinogenesis

Because CCR2 is expressed by non-bone marrow- as well as bone marrow-derived cells, we explored the contribution of CCR2-expressing non-bone marrow- and bone marrow-derived

cells to this colon carcinogenesis by using bone marrow chimeric mice prepared between WT and $CCR2^{-/-}$ mice. Upon the combined treatment with AOM and DSS, $CCR2^{-/-}$ and WT mice transplanted with WT mouse-derived bone marrow cells, developed tumors to similar but at a higher level than either WT or $CCR2^{-/-}$ mice transplanted with $CCR2^{-/-}$ mouse-derived bone marrow (Fig. 2). These observations would indicate that CCR2-expressing bone marrow-derived cells but not non-bone marrow-derived cells were mainly responsible for tumor development in this model.

Reduction in AOM/DSS-induced expression of COX-2 in $CCR2^{-/-}$ mice

Mirroring the crucial roles of COX-2 in colon carcinogenesis, COX-2 mRNA expression and COX-expressing cell number were increased in WT mice later than 7 days after the initiation of DSS treatment (Fig. 3), as we previously observed (2). AOM/DSS-induced increases in COX-2 mRNA expression and COX-2-positive cell numbers, were depressed in the absence of CCR2 (Fig. 3A, C). Collectively, AOM/DSS failed to increase the expression of COX-2 in $CCR2^{-/-}$ mice.

Reduction of tumor formation by CCR2 antagonist administration

In order to delineate the role of the CCR2/CCL2 interactions in the progression phase of this colon carcinogenesis model, we administered CCL2 N-terminal deleted form (7ND)-expression vector, a CCR2 antagonist, after the three cycles of DSS intake, when multiple colon tumors have developed. When WT mice were treated with 7ND-expressing vector, the numbers and sizes of macroscopical tumors were markedly reduced (Fig. 4B, C). Concomitantly, the treatment with 7ND-expressing vector decreased the numbers of infiltrating macrophages and neutrophils (Fig. 4D, E). Moreover, 7ND administration reduced intracolonic COX-2 mRNA expression and COX-2 expressing cell numbers (Fig. 4F and data not shown). Moreover, 7ND treatment decreased intratumoral CD31-positive vascular areas significantly (Fig. 4G, H). Furthermore, 7ND treatment decreased β-catenin nuclear accumulation in the tumor cells (Fig. 4I) and cytokeratin 20-positive cell numbers (data not shown). Collectively, these observations would indicate that the CCR2/CCL2 interactions were crucially involved even in the progression phase after multiple tumors developed, by regulating COX-2-expressing inflammatory cell infiltration.

Discussion

Accumulating evidence suggests that the CCL2/CCR2 axis plays important roles in the pathogenesis of various diseases by regulating the infiltration of macrophages. Indeed, the intramuscular transduction of the mutant MCP-1 gene, 7ND, MCP-1 inhibitor, inhibited vascular remodeling in rats (1), atherosclerosis progression in mice (3), and ameliorated renal ischemia-reperfusion injury and renal fibrosis in mice (4, 5). Thus, 7ND may effectively block CCL2/CCR2 signaling and play a protective role in related diseases.

Chemokines contribute to tumor growth and progression and CCL2 is reported to be expressed by a variety of cancer types. CCL2 may exert its tumor promoting effects by recruiting macrophages, which are major sources of growth and angiogenic factors. Once secreted from colon adenoma cells, CCL2 can stimulate COX-2 expression, as well as PGE_2 and VEGF release from human macrophages (6). Simultaneously, CCL2 can exert growth stimulating effects on CCR2-expressing tumor cells in an autocrine manner. In addition, CCL2 has been reported to possess proangiogenic activity on CCR2-expressing endothelial cells (7).

In this study we demonstrated that CCL2 production was enhanced during the course of AOM/DSS-induced colon carcinogenesis. Moreover, blocking of the CCL2/CCR2 signaling could attenuate colon tumorigenesis by decreasing the numbers of infiltrating COX-2-expressing macrophages and neutrophils, leading to reduced neovascularization and β-catenin activation. Thus, targeting the CCL2/CCR2 axis may prove beneficial for patients with inflammation-associated cancers.

References

1. Egashira, K., Koyanagi, M., Kitamoto, S., Ni, W., Kataoka, C., Morishita, R., Kaneda, Y., Akiyama, C., Nishida, K.I., Sueishi, K., Takeshita, A. Anti-monocyte chemoattractant protein-1 gene therapy inhibits vascular remodeling in rats: Blockade of MCP-1 activity after intramuscular transfer of a mutant gene inhibits vascular remodeling induced by chronic blockade of NO synthesis. *FASEB J*. 14, 1974-1978, 2000.
2. Popivanova, B.K., Kitamura, K., Wu, Y., Kondo, T., Kagaya, T., Kaneko, S., Oshima, M., Fujii, C., Mukaida, N. Blocking TNF-α in mice reduces colorectal carcinogenesis associated with chronic colitis. *J. Clin. Invest.* 118, 560-570, 2008.
3. Ni, W., Egashira, K., Kitamoto, S., Kataoka, C., Koyanagi, M., Inoue, S., Imaizumi, K., Akiyama, C., Nishida Ki, K., Takeshita, A. New anti-monocyte chemoattractant protein-1 gene therapy attenuates atherosclerosis in apolipoprotein E-knockout mice. *Circulation*. 103, 2096-2101, 2001.
4. Furuichi, K., Wada, T., Iwata, Y., Kitagawa, K., Kobayashi, K., Hashimoto, H., Ishiwata, Y., Tomosugi, N., Mukaida, N., Matsushima, K., Egashira, K., Yokoyama, H. Gene therapy expressing amino-terminal truncated monocyte chemoattractant protein-1 prevents renal ischemia-reperfusion injury. *J. Am. Soc. Nephrol.* 14, 1066-1071, 2003.
5. Wada, T., Furuichi, K., Sakai, N., Iwata, Y., Kitagawa, K., Ishida, Y., Kondo, T., Hashimoto, H., Ishiwata, Y., Mukaida, N., Tomosugi, Matsushima, K., Egashira, K., Yokoyama, H. Gene therapy via blockade of monocyte chemoattractant protein-1 for renal fibrosis. *J. Am. Soc. Nephrol.* 15, 940-948, 2004.
6. Tanaka, S., Tatsuguchi, A., Futagami, S., Gudis, K., Wada, K., Seo, T., Mitsui, K., Yonezawa, M., Nagata, K., Fujimori, S., Tsukui, T., Kishida, T., Sakamoto, C. Monocyte chemoattractant protein 1 and macrophage cyclooxygenase 2 expression in colonic adenoma. *Gut*. 55, 54-61, 2006.
7. Salcedo, R., Ponce, M.L., Young, H.A., Wasserman, K., Ward, J.M., Kleinman, H.K., Oppenheim, J.J., Murphy, W.J. Human endothelial cells express CCR2 and respond to MCP-1: direct role of MCP-1 in angiogenesis and tumor progression. *Blood*. 96, 34-40, 2000.

Figure Legends

Figure 1. Tumor formation and inflammatory cell infiltration in WT and CCR2$^{-/-}$ mice after AOM and DSS treatment. (**A**) Schematic overview of the experimental procedures. (**B**) Macroscopical appearance of the colons. Colons were removed at day 56 from treated WT and CCR2$^{-/-}$ mice and representative results from 10 independent animals are shown here. (**C**) Tumor numbers. Colons were removed at day 56 to determine the numbers of macroscopic tumors. Results are presented as mean ± SD (n=10 animals). **, $p<0.01$ versus WT mice. (**D**) MCP-1/CCL2 gene expression in the colons of WT mice. The levels of CCL2 mRNA were quantified by real-time RT-PCR as described in Methods, and normalized to the level of GAPDH mRNA. *, $p<0.05$, **, $p<0.01$ versus untreated (control) mice. (**E, F**) The numbers of F4/80- (**E**) and Ly-6G- positive (**F**) cells were counted as described in Methods and are shown here. All values represent the mean ± SD (n=10 animals), *, $p<0.05$, **, $p<0.01$ vs. untreated (control) mice.

Figure 2. Colon tumor formation in bone marrow chimeric mice.
Bone marrow chimeric mice were generated and subjected to AOM and DSS treatment as described in Methods. Colons were removed at day 56 and the tumor numbers were determined macroscopically. The bars represent the median of each group; each symbol represents the tumor numbers of each animal group (n=4÷5), *, $p<0.05$, **, $p<0.01$; NS, not significant.

Figure 3. COX-2 expression in the colons.
(**A**) Quantitative RT-PCR was performed on total RNAs extracted from the colons at the indicated time points as described in Methods. The levels of COX-2 mRNA were normalized to the levels of GAPDH mRNA.*, $p<0.05$, **, $p<0.01$, vs. untreated mice. (**B, C**) Immunohistochemical detection of COX-2 expressing cells. Colons were obtained from WT mice at the indicated time points and immunostained with anti-COX-2 antibody as described in Methods. Representative results from 6 independent animals are shown in **B.** Original magnification, x 400. The numbers of COX-2 expressing cells are shown in **C** and expressed as mean±SD. *, $p<0.05$, **, $p<0.01$, vs. untreated mice.

Figure 4. The effects of 7ND vector injection on colon carcinogenesis.

(**A**) Schematic overview of 7ND administration. (**B**) The tumor numbers and sizes were determined macroscopically. The bars represent the median of each group. Each symbol represents the tumor numbers of each animal or the average size of the tumors of each animal. (**C**) Macroscopic evaluation of the tumors. Colons were removed on day 67 from WT mice, injected with 7ND or with empty plasmid. Representative results from 7 to 8 independent animals are shown here. (**D**) and (**E**) F4/80-positive macrophage (**D**) and Ly-6G-positive granulocytes (**E**) were enumerated as described in Methods. All values represent the mean $\pm$ SD (n=5 animals). *, $p<0.05$, **, $p<0.01$, vs. empty plasmid injected WT mice. (**F**) Quantitative RT-PCR analysis for COX-2 was performed on total RNAs extracted from the colons at the indicated time points as described in Methods. The levels of COX-2 mRNA were normalized to those of GAPDH mRNA. **, $p<0.01$, vs. empty plasmid injected WT mice. (**G, H**) Colon tissues were immunostained with anti-CD31 antibody as described in Methods. The vascular densities were determined as described in Methods and are shown in **G.** *, $p<0.05$ vs. empty plasmid injected WT mice. (**I**) The β-catenin nuclear localization ratio was determined as the ratio of the numbers of tumor nuclei with β-catenin localization to the total number of tumor nuclei per field. At least 5 randomly chosen fields at x 400 magnification were examined. All values represent the mean $\pm$ SD, *, $p<0.05$, vs. empty plasmid injected WT mice.

Figure 1

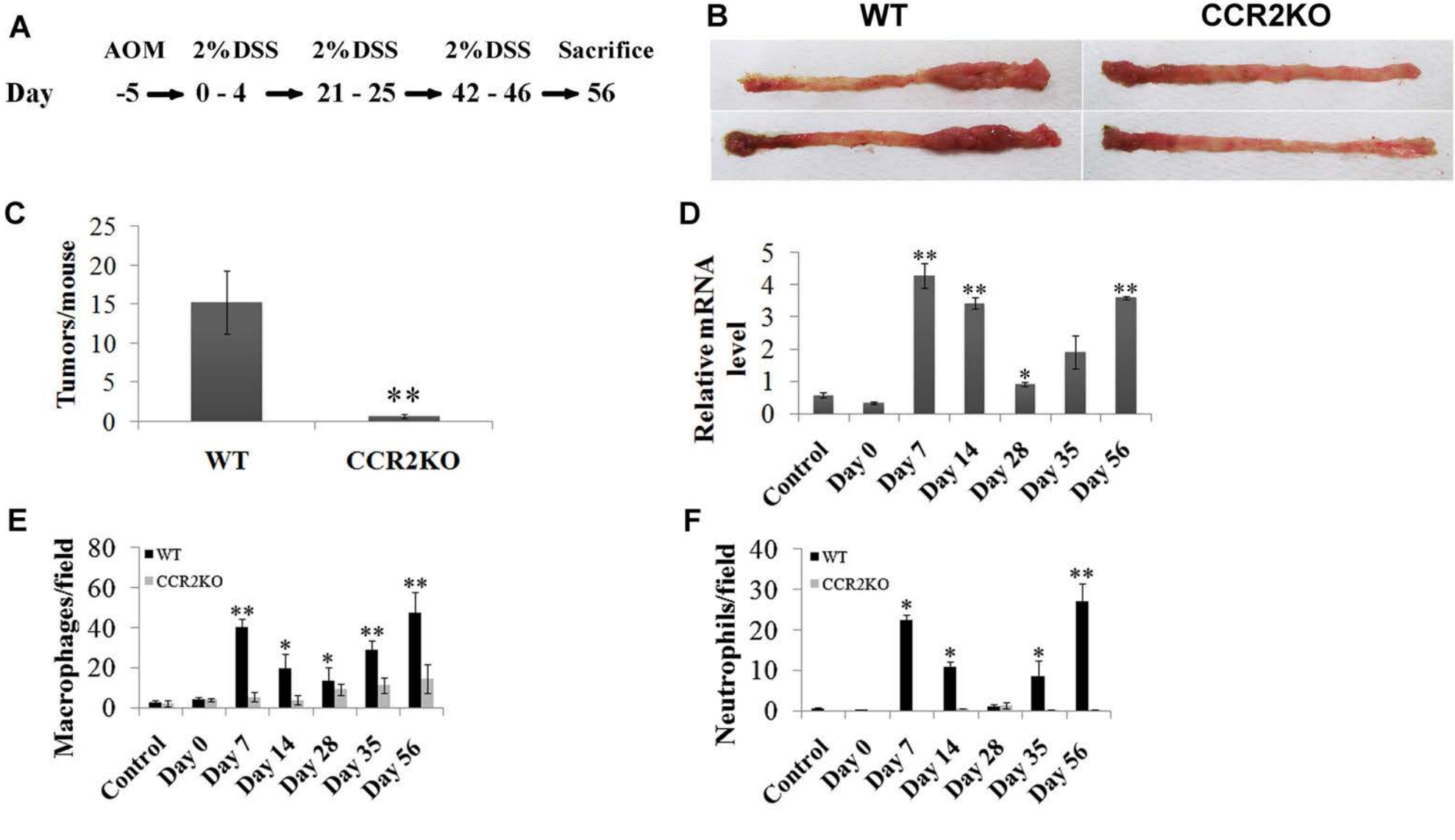
A
AOM
2% DSS
2% DSS
2% DSS
Sacrifice
Day
-5
0 - 4
21 - 25
42 - 46
56
B
WT
CCR2KO
C
Tumors/mouse
25
20
15
10
5
0
**
WT
CCR2KO
D
Relative mRNA level
5
4
3
2
1
0
**
**
*
**
Control
Day 0
Day 7
Day 14
Day 28
Day 35
Day 56
E
Macrophages/field
80
60
40
20
0
WT
CCR2KO
**
*
*
**
**
Control
Day 0
Day 7
Day 14
Day 28
Day 35
Day 56
F
Neutrophils/field
40
30
20
10
0
WT
CCR2KO
*
*
*
**
Control
Day 0
Day 7
Day 14
Day 28
Day 35
Day 56

Figure 2

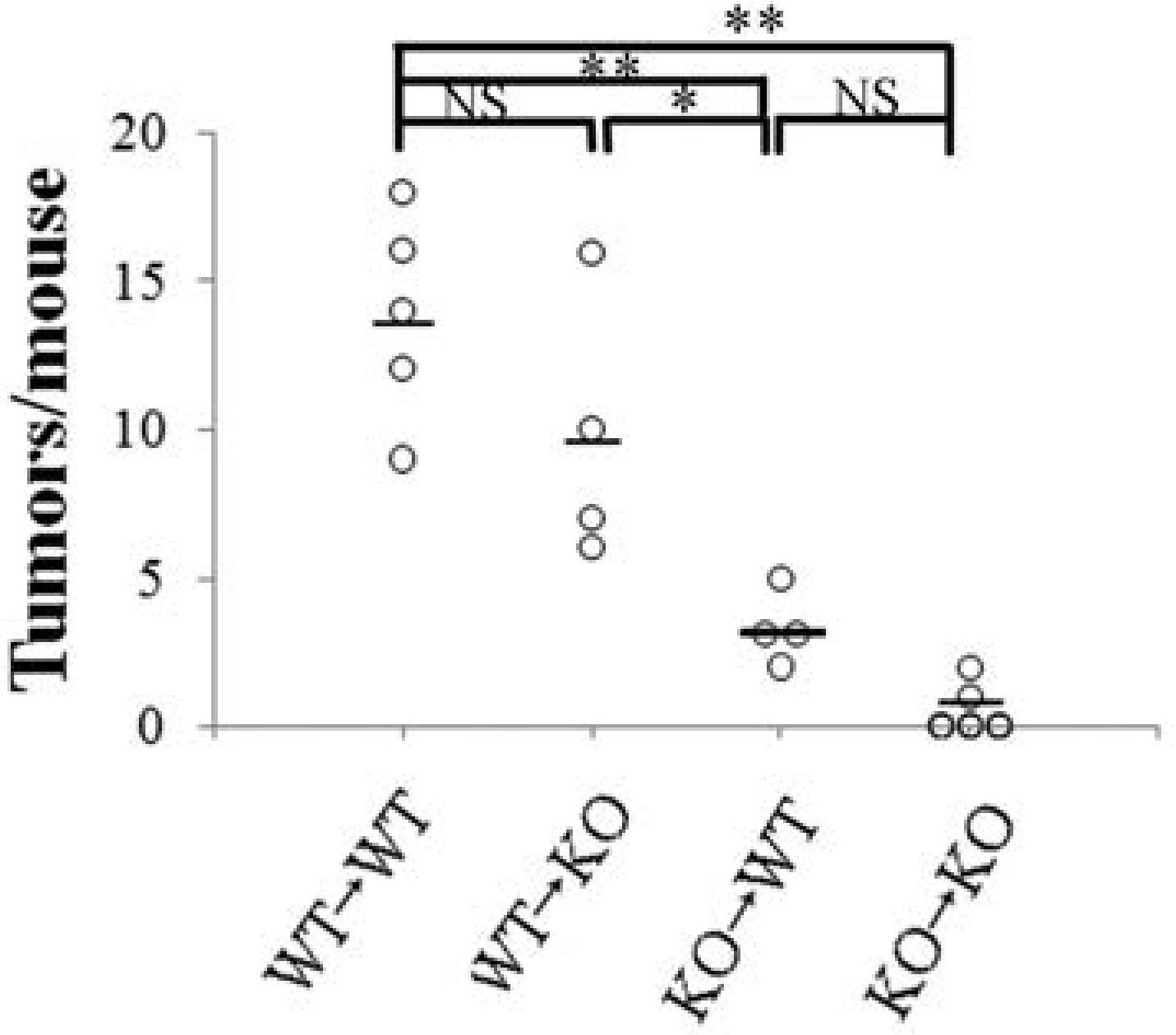

Figure 3

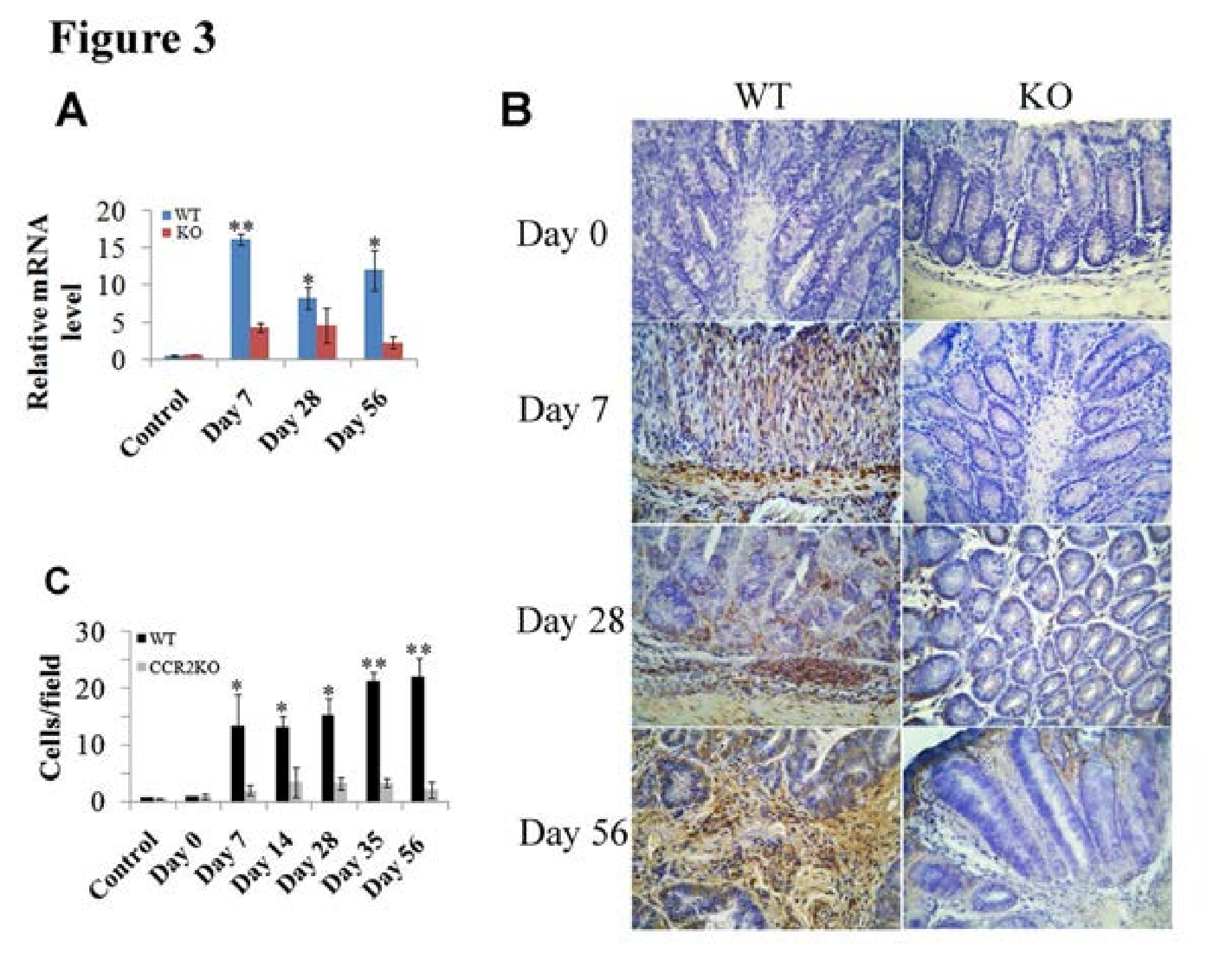
A
Relative mRNA level
20
15
10
5
0
WT
KO
**
*
*
Control
Day 7
Day 28
Day 56
B
WT
KO
Day 0
Day 7
Day 28
Day 56
C
Cells/field
30
20
10
0
WT
CCR2KO
*
*
*
**
**
Control
Day 0
Day 7
Day 14
Day 28
Day 35
Day 56

Figure 4

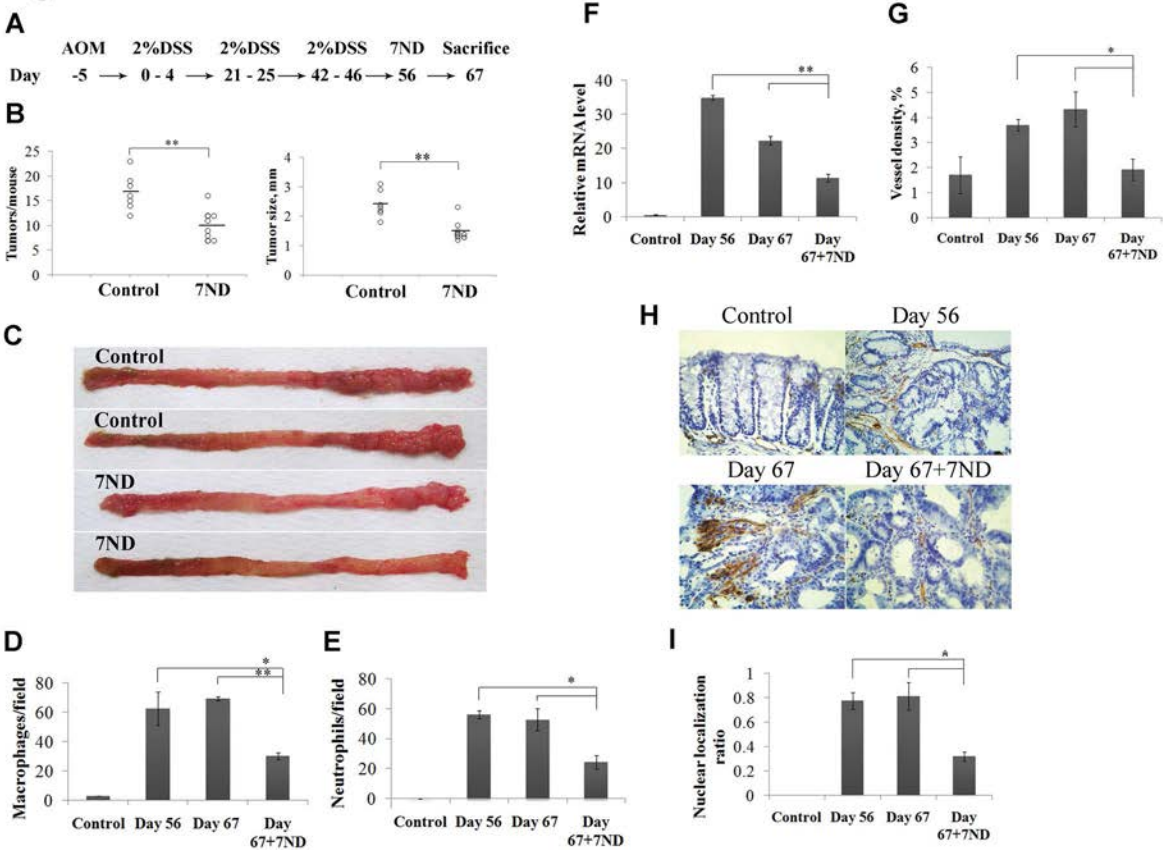
A
AOM
2%DSS
2%DSS
2%DSS
7ND
Sacrifice
Day
-5
0 - 4
21 - 25
42 - 46
56
67
B
Tumors/mouse
Tumor size, mm
**
Control
7ND
C
Control
Control
7ND
7ND
D
Macrophages/field
Control
Day 56
Day 67
Day 67+7ND
E
Neutrophils/field
F
Relative mRNA level
G
Vessel density, %
H
Control
Day 56
Day 67
Day 67+7ND
I
Nuclear localization ratio